Journal of Organometallic Chemistry 888 (2019) 29–36

Contents lists available at ScienceDirect

Journal of Organometallic Chemistry

journal homepage: www.elsevier.com/locate/jorganchem

Theoretical exploration of second-order nonlinear optical properties of mono- and bimetallic Pt(II) dithienylcyclopentene complexes: Ligands and photoisomerization effect

Yuan Zhang, Hong-Qiang Wang, Jin-Ting Ye, Xiang Li, Yong-Qing Qiu*

Institute of Functional Material Chemistry, Faculty of Chemistry, Northeast Normal University, Changchun, 130024, People's Republic of China

ARTICLE INFO

Article history:
Received 5 January 2019
Received in revised form
12 March 2019
Accepted 12 March 2019
Available online 16 March 2019

Keywords:
Pt(II) complexes
DFT
Second-order NLO response
Photoisomerization

ABSTRACT

On the basis of great diverse applications of nonlinear optical (NLO) materials, organometallic complexes have attracted considerable attention. In this paper, we present a detailed investigation on a series of Pt(II) dithienylcyclopentene(DTE)-based complexes via density functional theory method with the aim of evaluating their structures, electronic absorption spectra and first hyperpolarizabilities. The calculations demonstrate that the first hyperpolarizabilities can be enhanced by the introduction of quinolone into the complexes because of the enlarged spatial separation of electron density. However, Pt(II) complexes containing perfluorocyclopentene ring exhibit decreasing NLO response attributed to lower amount of charge transferred and short effective CT distance. The static first hyperpolarizabilities (β_{tot}) of monometallic Pt(II) complexes are larger than those of bimetallic Pt(II) complexes due to correlative mixed charge-transfer patterns. More importantly, the closed-ring (**1c**) complex comprising DTE unit exhibits the largest β_{tot} value approaching 144×10^{-30} esu, with the contrast over five times compared to corresponding open-ring due to the better π-conjugated delocalization and smaller HOMO and LUMO energy gap. In general, we envision our work will be beneficial for further rational design of DTE-containing Pt(II) complexes as high performance NLO materials.

1. Introduction

During the last two decades, compounds with large nonlinear optical (NLO) response have attracted extensive interest in view of their potential application involving optical computing, electro-optical devices as well as all-optical data processing technologies [1–6]. Since the earliest scientific publication reported the NLO properties of *cis*-1-ferrocenyl-2-(4-nitrophenyl)ethylene by Green et al. [7], organometallic complexes have emerged as a remarkable class of molecular NLO-phores owing to better thermal stability, ultrafast response times, stronger nonresonant responses and low dielectric constants in producing functional materials [8–12]. Besides, it has been demonstrated that the organometallic complexes have many additional electronic advantages over traditional organic counterparts on account of their low-energy charge-transfer transitions like metal-to-ligand charge transfer (MLCT), ligand-to-metal charge transfer (LMCT), metal-to-metal/intervalence charge transfer (MM/IVCT) excitations and the electronic distribution modulated by redox switching of the metal centre. The fundamental researches on NLO materials have been paid more attention to pursue large NLO response. Meanwhile, the researches for metal complexes with switchable NLO properties have another important topic.

In recent years, the switchable properties of photochromic materials such as magnetic properties, linear and nonlinear optical properties have been extensive investigated owing to their widespread applications in photo-optical switching devices and optical memory media [13–17]. In order to obtain pronounced switching effect, the compounds must be stable in multistate that exhibit different NLO responses, high switching speed and reversibility in various practical applications. The switching of NLO properties can be altered by specific procedures including photoisomerization, oxidation/reduction and protonation/deprotonation [18–24]. Among them, the dithienylethene(DTE) as a classic photoswitching unit has been widely studied due to the remarkable low photofatigue and thermal stability [25–27]. The photochromic moieties undergo reversible process between open and closed forms by UV light irradiation and visible spectral ranges, accompanied by

* Corresponding author..
E-mail address: qiuyq466@nenu.edu.cn (Y.-Q. Qiu).

https://doi.org/10.1016/j.jorganchem.2019.03.009
0022-328X/

significant changes of electrochemical and NLO properties [28–30]. Moreover, a number of efforts have been devoted to theoretical investigations and synthesis of metal complexes with DTE-derived active component with desired NLO switchable properties [31–36]. The first example of zinc(II) DTE photochromic dipolar complexes have been reported by Aubert group [31]. They described that the $\mu\beta$ values of closed-ring are larger than those of open-ring isomers. Samoc et al. synthesized a binuclear Ru(II) alkynyl complex with a diarylethene bridge, which shows six switchable states and possesses distinct NLO behaviors [36]. Additionally, The Pt(II) combined to DTE-based ligands complexes have been paid attention to their NLO properties by experiments or theoretical calculations [37–42]. Jacquemin with co-workers contributed a series of researches on the NLO properties of cyclometalated Pt(II) DTE-containing complexes. In 2014, they reported the first example of photochromic cyclometalated Pt(II) complexes as switchable NLO polymer films with better NLO contrast. The electron-donor group ($D = NMe_2$) introduction into Pt(II) complex can provide good second-order NLO response [39]. In addition, the novel cyclometalated Pt(II) (phbpy) DTE-based complexes with sequential double nonlinear optical switch have been investigated in detail by the EFISH technique and theory. The values of $\mu\beta_{EFISH}$ for studied complexes are enhanced by protonation and then increased upon photocyclization owing to the longer charge-transfer distance and higher dipole moment [40]. As the extension of mononuclear photochromic Pt(II) complexes, they synthesized two covalently linked bimetallic Pt(II) complexes, where the two metal fragments are diversely framing the same DTE core and the quadratic NLO properties were characterized via EFISH method. This work illustrates an enhanced photomodulation of the NLO response in the DTE closed form. The value of $\mu\beta_{EFISH}$ for complex Pt(II)-acetylide moieties connected to the reactive atoms is slightly larger than that previously reported monometallic Pt(II) complex in open form [41]. Recently, a series of functionalization Pt(II) complexes where the DTE unit is connected at the para-position of the central benzene of the ligand were also synthesized and characterized in both solution and thin films. The remarkable enhancement of the second-order NLO response upon ring-closing is due to the extended π-delocalization and decrease of the HOMO−LUMO gap. However, the substitution of perfluorocyclopentene group does not clearly affect the quadratic NLO activity [42]. The development of these materials may be expected to result in novel switchable NLO applications. In previous work, our group systematically studied the NLO properties of a series of Pt(II) (acetylacetonate) (2,2′-thiophenylpyridine) derivatives. It is mainly discussed that multiple relationships with the number of thiophene rings and tuning electron-withdrawing substituents accompanied with adjustment of NLO response [43]. Recently, Gamez et al. have synthesized a series of novel Pt(II) complexes with photoresponsive DTE ligands and assessed the properties of potential biomedical properties [44]. Intriguingly, the notable geometry changes of these Pt(II) DTE-based complexes from nonconjugated form(open-ring) to conjugated state (closed-ring) will result in the switchable NLO responses. Stimulated by the excellent previous works, we carried out density functional theory (DFT) to research the electronic structures, electronic absorption spectra and the quadratic hyperpolarizabilities values of the Pt(II)-coordinated DTE complexes.

In this work, the mono- and bimetallic complexes were comparatively studied. The various kinds of ligands on the bimetallic complexes were further explored with the aim to rationalize the relationship between the structure and NLO properties. The closed-ring complexes are named as **1c**–**5c** and the corresponding open forms are **1o**–**5o** in the present paper. We aimed at: (i) elucidating the differences of mono- and bimetallic complexes on the second-order NLO responses; (ii) investigating the effects of various ligands and photoisomerization on geometrical structures, the charge transfer (CT) properties as well as first hyperpolarizabilities. We hope this work would provide a theoretical and experimental guidance for exploiting other novel NLO materials.

2. Computational details

All calculations in this paper were carried out by using Gaussian 09W program package [45]. On the basis of experimental data [44], the geometries of **4o** complex were optimized in DFT framework by using B3LYP [46,47] and PBE1PBE hybrid functionals [48,49]. The 6-31G(d) all-electron basis set was employed for nonmetal elements, whereas transition metal Pt(II) used SDD basis set with the Stuttgart Dresden effective core potentials. The crystallographic data and calculated geometric parameters of **4o** are given in Table S1 (Supporting Information), and the corresponding atom labels are displayed in Fig. S1. The geometric parameters of the all complexes have been optimized by using the PBE1PBE functional, and no symmetry restriction was offered in structure optimization process. Furthermore, frequency calculations were applied to verify that the structures are minima on the energy surface. The bond length alternation (BLA) value is used to measure the degree of delocalization and defined as equation

$$\mathrm{BLA} = \frac{1}{N}\sum d(\mathrm{single}) - \frac{1}{M}\sum d(\mathrm{double}) \quad (1)$$

Here, M and N indicate the number of double and single bonds along the conjugation path respectively, while d means bond length. With respect to the calculation of the polarizability and hyperpolarizability, one option is to use the derivates either analytically or numerically. In this paper, the static first hyperpolarizabilities (β_{tot}) were obtained by analytical third energy derivatives owing to more efficient and less expensive.

The β_{tot} was calculated by the following equation:

$$\beta_{tot} = (\beta_x^2 + \beta_y^2 + \beta_z^2)^{\frac{1}{2}} \quad (2)$$

where

$$\beta_i = \beta_{iii} + \frac{1}{3}\sum_{i\neq j}(\beta_{ijj} + \beta_{jij} + \beta_{jji}) \quad (\mathrm{i, j} = \mathrm{x, y, z}) \quad (3)$$

In recent years, range-separated exchange functionals have been extensively employed and more suitable to evaluate extended compound. The CAM (Coulomb-attenuating model) was proposed as an applicable method for the first hyperpolarizability, which contains 65% and 19% of long- and short-range HF exchange [50,51]. The ωB97XD functional is the latest functional from Head-Gordon and Chai [52], while the hybrid functionals M06-2X containing HF exchange weighting 54% is an excellent for the first hyperpolarizability [53,54]. The CAM-B3LYP, ωB97XD and M06-2X functionals were adopted to calculate the β_{tot} values in this paper. It is well-known that the choice of basis set is essential to obtain reliable results. Five Pople's basis sets 6-31G(d), 6-31 + G(d), 6-31 + G(d,p), 6−31++G(d,p) and 6−311++G(d,p) at the CAM-B3LYP level for **1c** complex were chosen to assess the effect of the basis set. Owing to the high computational cost, the SDD basis set was selected for transition metal Pt and the nonmetal elements used 6-31 + G(d) basis set.

Time-dependent DFT (TDDFT) is one of the most prevalent tools to understand the NLO behaviors in quantum chemistry because of its efficiency and accuracy [55–57]. Choosing a suitable DFT functional is important for computing absorption spectra. As a result, the calculations of the excitations were investigated by the TDDFT

method at the B3LYP/6-31G(d)/SDD level, since the B3LYP functional is in satisfactory agreement with experimental values [44]. The solvent effect has been considered by the polarizable continuum model (PCM) in dichloromethane solvent [58]. To evaluate the charge transfer (CT) abilities process, the CT parameters containing the amount of transferred electrons (q^{CT}), the corresponding effective CT distance (d^{CT}) and the t index definited as the degree of $\rho^{+}(r)$ and $\rho^{-}(r)$ based on the total densities for the ground and excited states are calculated. The larger t index indicates the little overlap between the electron-accepting and electron-donating regions exists.

3. Results and discussion

3.1. Geometrical and electronic structures

Two hybrid functionals B3LYP and PBE1PBE at the 6-31G(d) basis set for nonmetal atoms and SDD basis set for Pt atom were chosen to optimize the geometrical structure of **4o** derived from crystal structure. The results illustrate that the geometrical parameter obtained by PBE1PBE functional are in well accordance with the crystal data [44], indicate the geometrical calculations are reliable. Therefore, the geometry structures of open- and closed-ring complexes have been applied at PBE1PBE/6-31G(d)/SDD level. The studied complexes structures are shown in Fig. 1. The optimized calculations display clear differences on two thiophene of DTE unit in photoisomerization process. The dihedral angel between the two thiophene rings of **1o** complex is measured to be 120.4°, in contrast, the dihedral angle of closed-ring complex nearly increase to 170.6°. The geometrical changes are affected by two rotatable thiophene rings of DTE units. It is relatively distinct changes on C1-C2 bonds length about 0.09 Å between open- and closed form. The conformation changes are analogical in other complexes. The geometry variations from the nonplanar DTE unit of open complexes to conjugated closed form may inevitably influence the NLO responses. In addition, the BLA value regarded as a quantitative tool to assess the degree of π-conjugation for the molecule with conjugated bonds were investigated, thus the related single and double bond in the blue bold are collected in Fig. 1. As demonstrated shown Table 1, the BLA values of open-ring complexes are higher than those of the corresponding closed-ring complexes. It means stronger π conjugation structure in the closed-ring form when irradiated in the UV/visible, which is relevanted to large hyperpolarizability NLO responses.

The discrepancy in the geometry may give rise to different electronic structure. The frontier molecular orbitals (FMOs) are usually applied to reveal the relationship between the electronic properties and geometric structures. The HOMO−LUMO energy gap (E_{gap}) is an important parameter properly affect the NLO responds (Table 1). It is found that the LUMO energy complex **1c** is lower than that of **1o**, whereas the HOMO energy is higher than that of complex **1o**. Therefore, it can be seen that the E_{gap} value of **1c** is smaller than that of complex **1o** by ~1.39eV. Bear in mind, a lower HOMO−LUMO energy gap would be beneficial to larger NLO response. The HOMO and LUMO energy gaps can be obviously narrowed in closed-ring systems, further predict the β_{tot} values may gradually increase.

3.2. Static first hyperpolarizabilities

As aforementioned, the variations of geometry and electronic structures may inevitably affect the NLO properties. For the sake of confirming the accuracy of β_{tot} results, we have adopted three functionals (M06-2X, CAM-B3LYP and ωB97XD) for assessing the effect of DFT functional on the NLO response. The β_{tot} values together with the components values obtained by three functionals for studied complexes are listed in Table S2 and plotted in Fig. 2, respectively. In all case, the β_{tot} values of M06-2X give relatively large values compared to the CAM-B3LYP results, providing a consistent trend for investigating the qualitative second-order NLO properties. In addition, the relational studies show that the CAM-B3LYP functional was proposed as a suitable approach to predict the first hyperpolarizability owing to its semiquantitative accuracy [59]. Hence, we only take the calculated β_{tot} values of CAM-B3LYP functional as example to shed light on second-order NLO responses for current systems. Moreover, a suitable basis set is important to calculate the first hyperpolarizability of all studied complexes. Several pople's basis set (6-31G(d), 6-31 + G(d), 6-31 + G(d,p), 6−31++G(d,p) and 6−311++G(d,p)) at the CAM-B3LYP level for **1c** complex have been used and listed in Table S3. It is noted that the diffuse functions and polarization have a little influence on the NLO response. Taking the computation costs into

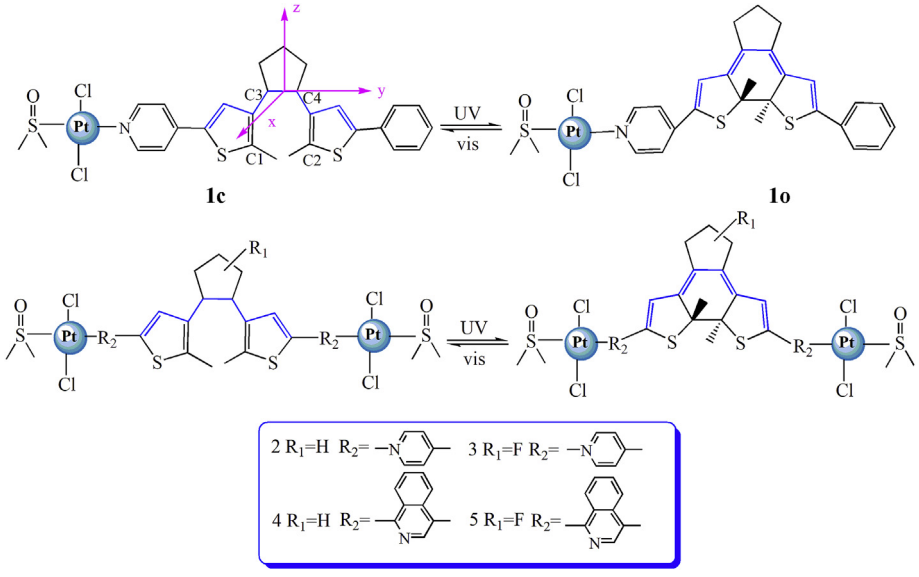

Fig. 1. Calculation models of the studied complexes.

Table 1
HOMO and LUMO energy levels, H-L gap (E_{gap}) and BLA values (Å) of all studied complexes.

Complexes	HOMO	LUMO	E_{gap}	BLA
1c	−5.93	−2.06	2.48	0.067
2c	−6.42	−2.3	2.49	0.068
3c	−6.51	−2.57	2.48	0.065
4c	−5.97	−2.25	2.45	0.071
5c	−6.40	−2.42	2.49	0.066
1o	−5.13	−2.65	3.87	0.082
2o	−5.60	−3.11	4.12	0.080
3o	−6.16	−3.68	3.94	0.078
4o	−5.17	−2.72	3.72	0.083
5o	−5.73	−3.24	3.98	0.081

account, the CAM-B3LYP/6-31 + G(d)/SDD was a proper level to calculate the first hyperpolarizabilities (Table 2). For studied systems, the origin of the cartesian coordinate system is located at the middle of the C–C bond in cyclopentene ring and the horizontal y-axis pointing to phenyl or quinolone moieties.

In the present study, we focused on analyzing the magnitude of first hyperpolarizabilities. As displayed in Table 2, it is clearly seen the computed β_{tot} values of closed-ring increase as the order β_{tot} (**3c**) < β_{tot} (**5c**) < β_{tot} (**2c**) < β_{tot} (**4c**) < β_{tot} (**1c**). The results illustrate the same trend in the open-ring complexes. In addition, the closed-ring **1c** complex possesses the largest β_{tot} value of 144.86×10^{-30} esu, which is about 3.1 times as large as the **2c**. Analogously, the β_{tot} value of **1o** complex is maximum value (26.78×10^{-30} esu), almost 2.1 times with respect to **2o**. It indicates that bimetallic Pt(II) complexes result a significant decrease of the β_{tot} values. Note that modulating DTE-based ligands of these complexes, the closed-ring complexes have been selected as prototype to discuss first hyperpolarizabilities in more detail. Complexes **2c** and **4c** can present the β_{tot} values as 46.55×10^{-30} esu and 54.1×10^{-30} esu, which are about ~2.3 and ~2.2 times as large as those of **3c** and **5c**, respectively. The results suggest that Pt(II) complexes containing a central perfluorocyclopentene ring exhibit inevitably decrease the second-order NLO response. Moreover, the magnitude β_{tot} values of complexes **4c** and **5c** are much larger than those of **2c** and **3c**. It suggests that adding quinolone moiety is more helpful to enhance the β_{tot} value. To sum up, modifying various DTE-based ligands can be considered as effective method to tune second-order NLO response.

In an attempt to further understand the origin of the second-order NLO properties, perspective was considered from the tensorial components. As shown in Table 2, the diagonal tensorial components β_{yyy} (for system 1) is the dominant one, inevitably leading to the large β_y total components owing to CT transfer occurring along y-axis. In the case of other pairs of **2**–**5**, a single hyperpolarizability independent tensor component β_z is the main contribution for β_{tot}. The off-diagonal β_{yyz} tensorial component is the dominant one leading to the largest β_z total component, indicate the CT transfer occurs at yz-plane. To further explore more intuitive information about the contribution to β values, the first hyperpolarizability density analysis which is the spatial electronic contribution to the first hyperpolarizabilities have been performed in this section. The β density and ρ_{yy} are numerically calculated from the second-order derivative of electron density with respect to an applied electric field and defined according to eq (4)

$$\rho_{yy}^{(2)}(r) = \frac{\partial^3 \rho(r)}{\partial F_y^2}|_{F=0} \tag{4}$$

and the β values are given by eq (5):

$$\beta_{yyy} = \int -\rho_{yy}^{(2)}(r) y dr \quad \beta_{yyz} = \int -\rho_{yy}^{(2)}(r) z dr \tag{5}$$

Since the β_{tot} values of open-a and closed-ring complexes are consistent with the same trend, we only focus on the β densities of closed-ring complexes. The $\rho_{yy}^{(2)}(r)$ corresponding to β_{yyy} is the most crucial component of β_{tot} in complex **1c**, whereas $\rho_{yy}^{(2)}(r)$ is related to off-diagonal β_{yyz} and the main component for complexes **2c-5c**. The plots of $-y\rho_{yy}^{(2)}$ and $-z\rho_{yy}^{(2)}$ together with corresponding β_{tot} values of the closed-ring complexes at the CAM-B3LYP/6-31G+(d)/SDD level have been provided in Fig. 3. The local contribution is decomposed into a pair of positive (pink region) and negative (yellow region) parts. It is clearly observed that the region of positive contributions dominate the $-y\rho_{yy}^{(2)}$ and $-z\rho_{yy}^{(2)}$ function spreading all over the complexes and prevailing over corresponding negative parts. As a consequence, the components β_{yyy} and β_{yyz} present the relative large positive values. As visualized in Fig. 3, complex **1c** has larger area of positive β density, providing a rather large positive β_{yyy} value (140.4×10^{-30} esu). On the other side, with regard to quinoline-containing complexes **4c** and **5c** show the area of positive contribution amplitude going much larger than those **2c** and **3c**. It indicates the off-diagonal β_{yyz} values for complexes **4c** and **5c** would be undoubtedly larger the positive β_{yyz} values with respect to **2c** and **3c**. Therefore, β-density distributions can be deemed as an efficient auxiliary method to assess the relative amplitudes of the β_{tot} values.

Coming the photoisomerization influence on first hyperpolarizabilities results, the DTE unit undergoes reversible interconversion between a nonconjugated form and π-conjugated

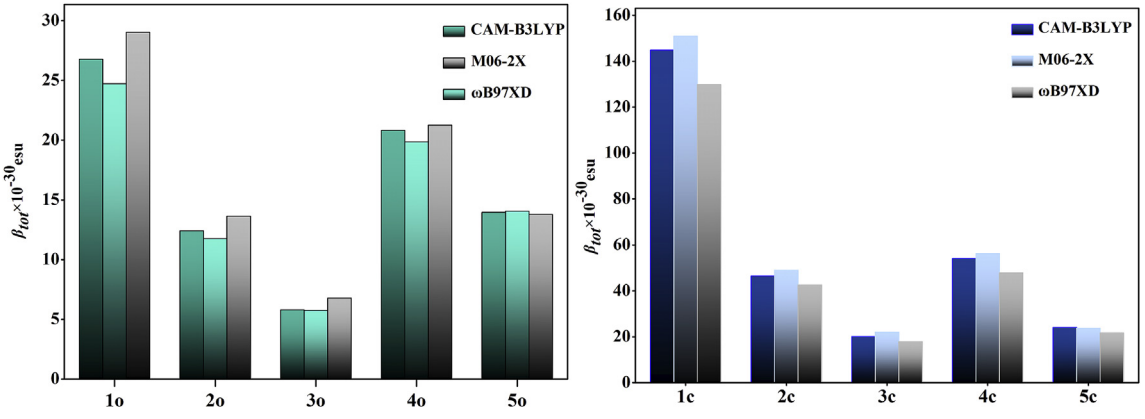

Fig. 2. Relationship between the β (10^{-30} esu) values of the open-ring and the closed-ring complexes computed at various levels of theory.

Table 2
The main individual components of first hyperpolarizabilities and total first hyperpolarizabilities (10^{-30} esu) of the studied complexes calculated at CAM-B3LYP/6-31 + G(d)/SDD level.

Complexes	β_x	β_y	β_z	β_{yyy}	β_{yyz}	β_{tot}
1c	−5.1	142.6	25.3	140.4	23.0	144.9
2c	8.6	−2.0	45.7	−7.1	41.9	46.6
3c	3.7	−3.3	19.5	−4.5	16.9	20.1
4c	10.6	−1.3	53.1	−2.7	43.2	54.1
5c	−4.6	0.7	23.7	0.3	14.8	24.1
1o	−8.4	23.6	9.4	20.0	6.4	26.8
2o	−2.9	−2.4	11.8	−3.0	9.7	12.4
3o	−2.4	0.5	5.2	1.0	2.7	5.8
4o	−1.8	−2.1	2.9	−0.6	−6.8	20.8
5o	1.0	0.4	13.9	0.7	5.0	14.0

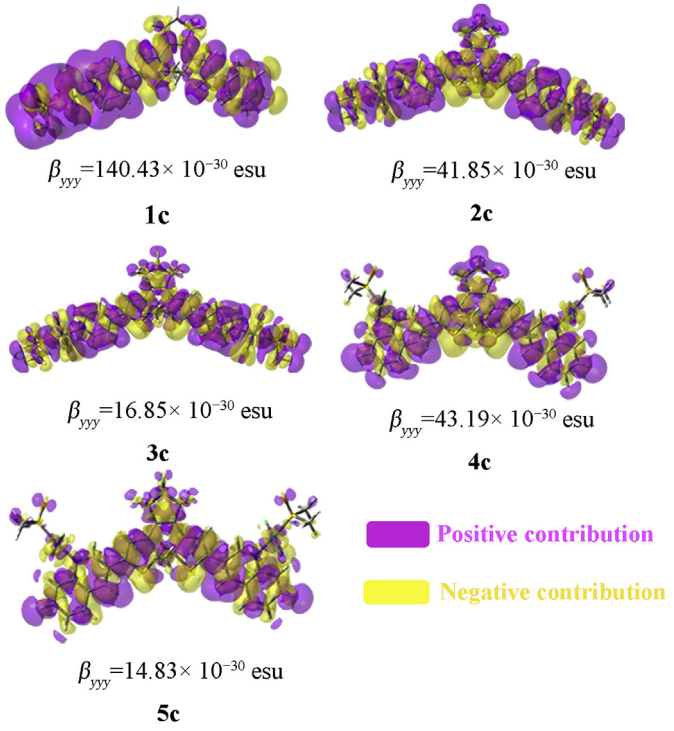

Fig. 3. Primary tensorial components of complexes **1c**–**5c** (pink color represents positive contribution, while yellow color represents negative contribution). (For interpretation of the references to color in this figure legend, the reader is referred to the Web version of this article.)

closed form, accompanied by the β_{tot} values are larger than those of the corresponding open-ring complexes. These improved β_{tot} values for closed-ring complexes are due to the smaller BLA values, as is mentioned previously about BLA values. It proposes that the photoisomerization result in a large enhancement of the second-order NLO property. It's worth noting the switch ratios of the open-ring and closed-ring are in the range of 1.7–5.4 times. The multiplying factor for system 1 ($\beta_{\mathbf{1c}}/\beta_{\mathbf{1o}}$) is 5.4 times show better switching properties on second-order NLO coefficients. Thereinto, monometallic Pt(II) DTE-based complex with the efficient second-order NLO switching response might be probable candidates for switchable NLO materials. The β_{tot} of bimetallic Pt(II) complex **2c** is 46.55 × 10^{-30} esu, which is ~3.7 times as large as those open form. The difference on the β_{tot} values between open form **5o** and closed form **5c** is the smallest, which is $\beta_{tot}(\mathbf{5c}) = 1.7\beta_{tot}(\mathbf{5o})$. Likewise, the β_{tot} value of closed form **3c** has only slightly increase compared to **3o**. There are slight enhancement of the $\beta_{tot}(c)/\beta_{tot}(o)$ values with Pt(II) complexes containing a central perfluorocyclopentene ring. In summary, photoisomerization effect play a beneficial role in tuning the NLO switch response on monometallic Pt(II) DTE-containing complexes.

3.3. Absorption spectrum

For the sake of elucidating the origin of the second-order NLO responses for open- and closed-ring complexes, we present herein the UV–vis absorption spectra for these complexes in dichloromethane solution by TD-DFT methodology. To verify the computational results reasonably, various functionals (TD-B3LYP, TD-PBE1PBE, TD-ωB97XD and TD-BHandHLYP) with the same basis set were carried out to simulate the experimental electronic absorption spectra (Fig. 4). It is found that the simulated UV–vis absorption spectrum received from B3LYP contains one intense high-energy absorption at 292 nm along with weak low-energy absorption at 341 nm, which are satisfactory agreement with the experimental data (286 nm and 322 nm) respectively. Hence, a detailed discussion has been performed the crucial transitions in dichloromethane solution with the TD-B3LYP/6-31G (d)/SDD method. To confirm the definition of crucial excited state is credible, we adopted the sum-overstate (SOS) method at the TD-B3LYP level in the framework of SOS perturbation theory. SOS method can preferably provide the contribution to the hyperpolarizabilities from various excited states. In this paper, a total of 100 states were used to adequately acquire the converged β_{tot} values (Fig. S2). The principal electronic transition parameters corresponding containing absorption wavelengths (λ), oscillator strengths (f_{os}), the excitation energies (ΔE_{ge}), associated orbital transitions and electron density difference maps (EDDM) of the crucial excited state are compiled in Table S4. The purple color area delegates the electron acceptor, and the blue color region represents the electron donor. The relevant simulation absorption spectra are shown in Fig. S3.

As depicted in EDDM, open-ring complex **1o** mainly consists of two absorption bands. Both the S1 (406 nm) and S9 (315 nm) states provide dominant contribution to the β_{tot} value. The simulated absorption spectrum exhibits one high-energy absorption peak absorbing at 406 nm along with an additional weak low-energy transition absorbing at 315 nm, which are described by the HOMO→LUMO (98%) and HOMO-3→LUMO (93%) excitations, respectively. The electronic transition state S1 absorbing at 406 nm, the HOMO is delocalized through benzene and DTE fragments, whereas the LUMO is located on the metal Pt(II) and pyridine groups. The CT pattern can be designated as intraligand charge transfer (ILCT) transition from benzene ring to pyridine section. Perception of corresponding EDDM reveal that S9 excitation can attribute to a mixed MLCT transitions of Pt(II) atom and pyridine, ILCT from DTE part to pyridine group and a small ligand-to-ligand charge transfer (LL'CT) from the ligand chlorine to pyridine section. As for **1c**, the electronic transition state S1 absorbing at 662 nm is formed by the HOMO→LUMO transition, which can be viewed as ILCT transition from the DTE moieties to pyridine ring. According to the EDDM, the S12 electronic transition is categorized as the mixture of LL'CT from ligand chlorine to pyridine, combined with CT trend from benzene to the DTE linker and pyridine moieties and larger MLCT transitions of Pt(II) atom and pyridine. Intriguingly, the difference of β_{tot} values between open- and closed form is pronounced for all studied complexes. As noted in Fig. S3, remarkable red-shifted from 406 nm to 662 nm are observed in the **1c** complex compared with **1o**. Moreover, the low-energy absorption bands of closed-ring complexes are bathochromic-shifts with respect to the relevant electronic transitions in the simulated spectra of open-ring complexes. This phenomenon suggests that closed-ring complexes may give rise to relatively high first

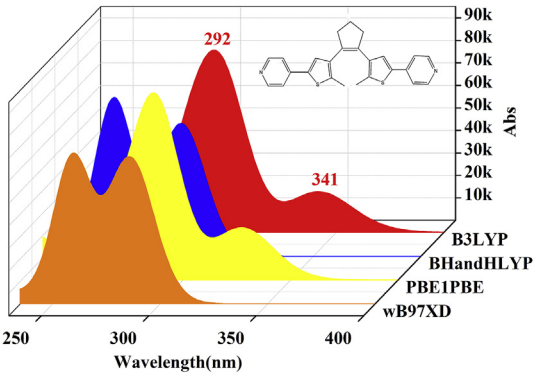

Fig. 4. Comparison of the absorption spectra of ligand computed by various functionals of theory.

hyperpolarizabilities values, which is also coincident with the HOMO and LUMO energy gap.

We are interested the influence of various ligands on the second-order NLO properties. The UV–vis spectra of closed-ring complexes **2c-4c** are preliminarily analyzed in parallel. As depicted in Table S4, the simulated absorption spectrum of **2c** exhibits the electronic transition state S2 absorbing at 475 nm due to HOMO→LUMO+1 (76%) and HOMO-1→LUMO (22%) transition. The band may be mainly assigned as ILCT [π(DTE)→π*(pyridine)]. The band absorbing at 424 nm is assigned as main contribution ILCT from DTE to pyridine part. Significantly, the mixed CT pattern within the **1c** inevitably results in the relatively larger the degree of charge transfer than **2c**. Hence, it is confident in attributing the larger β_{tot} value of system **1** than system **2** to their apparent distinct of charge transfer form. Complex **3c** has been associated with excited S1 and S5 states one middle-energy electronic transition absorbing at 414 nm and a low-energy electronic transition at 685 nm respectively, and both of the two states can be assigned as ILCT. Note that charge transfer patterns of **3c** have been observed quite similar to that of **2c** in EDDM. The S1 (673 nm) and S2 (549 nm) states of **4c** complex are mainly contributed by the HOMO→LUMO (100%) and HOMO→LUMO+1 (98%) transition respectively, which provide dominant contribution to the β_{tot} value. Both of them can be viewed as ILCT mainly from the middle DTE part to the two quinolone sides. Moreover, **4c** obviously enlarge spatial separation of electron density compared with **2c**. To sum up, this phenomenon would be conducive to further research that various ligands of metal complexes can affect the degree of charge transfer, which plays a crucial part in the modification of the second-order NLO response.

As is well known, the obvious charge transfer is the indispensable requirement to attain high NLO response. Motivated by this, taking closed-ring complexes as typical, the CT parameters including the magnitude of CT (q^{CT}), the relevant effective CT distance (d^{CT}) and t parameter for the ground state and the excited state are quantitatively evaluated. With a view of visualizing the spatial extent and overlap between the regions of density diminution and increment, the centroids of charge for studied complexes are plotted in Fig. 5. Taking the slight difference on CT patterns of complexes **2c** and **3c** into consideration, the corresponding parameters are analyzed primarily. The amount of q^{CT} for complex **2c** is 0.485 |e|, which is slightly larger than that of **3c** (0.469 |e|), and the corresponding d^{CT} value is decreased from 0.404 Å to 0.256 Å. It is obvious that transition of complex **2c** present relative stronger CT character than **3c**, thus leading to more effective NLO response. Indeed, complexes **2c** and **4c** show the longer charge transfers length as well as the larger t index assessing

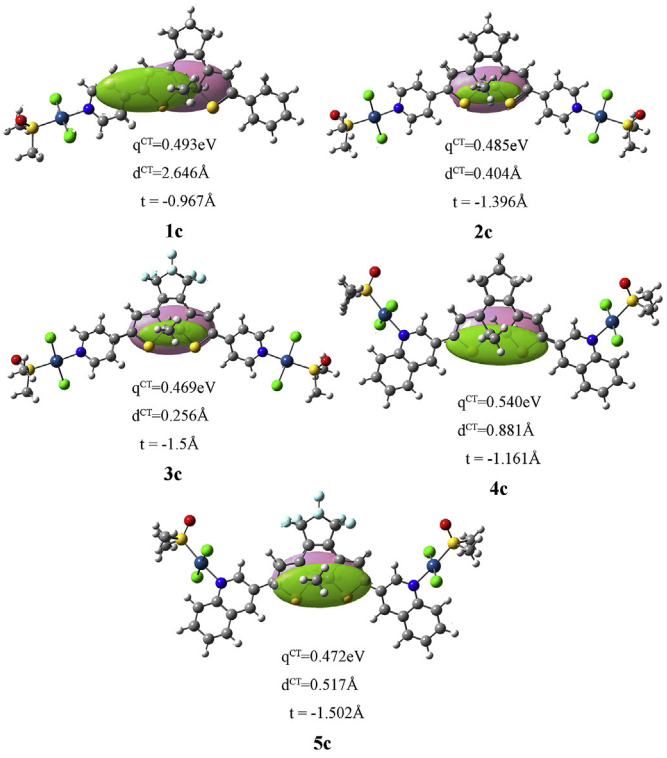

Fig. 5. Centroids of charge for the closed-ring complexes (pink and green zones correspond to electron density depletion and enhancement zones respectively). (For interpretation of the references to color in this figure legend, the reader is referred to the Web version of this article.)

the charge separation extent. These quantitative data show that Pt(II) dithienylcyclopentene–based complexes have stronger CT character, accompanied by better second-order NLO properties. It is worth mentioning the closed-ring complex **1c** with the larger amount of charge ($q^{CT} = 0.493$ |e|), the largest associated charge transfer distance ($d^{CT} = 2.646$ Å) as well as the smaller overlap, suggesting that complex **1c** has a maximum CT and obvious spatial charge separation, which is in reasonable agreement with mentioned previous regarding the first hyperpolarizability analysis. Considering the above discussions, it is very meaningful that the quantitative measures of the magnitude and length of the CT process are in favor of the modification of the degree charge transfer. The monometallic Pt(II) complexes are predicted to have the superior second-order NLO responses.

3.4. Frequency-dependent first hyperpolarizabilities

It is necessary to decide frequency-dependent properties theoretically result from experimental measurements of β_{tot} values usually include oscillating electric fields. The effect of dispersion behaviors on the second harmonic generation (SHG) β (-2ω; ω, ω) and the electro-optical pockels effect (EOPE) β (-ω; ω, 0) of **1** and **2** systems have been calculated by using coupled perturbed density function theory (CPDFT) method at CAM-B3LYP/6-31 + G*/SDD level. Three optical wavelengths with 1340 nm, 1460 nm and a nonresonant wavelength of 1907 nm were employed to show the dispersion contribution to the NLO response in Table 3. According to the data, it is visualized that the magnitude of β (-2ω; ω, ω) and β (-ω; ω, 0) are enhanced with increasing frequency. Moreover, the calculated frequency-dependent β (-2ω; ω, ω) shows the largest frequency dispersion, thus β (-ω; ω, 0) values are larger than those of corresponding static β_{tot} values, which indicates the frequency-

Table 3
The estimated values of β(-2ω; ω, ω) and β(-ω; ω, 0) (10^{-30} esu) at specific frequencies at the CAM-B3LYP/6–31 + G(d) level.

Complexes	1340nm		1460nm		1907nm	
	β_{SHG}	β_{EOPE}	β_{SHG}	β_{EOPE}	β_{SHG}	β_{EOPE}
1c	568.5	199.5	405.9	188.7	240.5	168.1
1o	38.7	29.9	36.3	29.4	31.7	28.2
2c	144.3	60.4	108.1	57.8	70.3	52.6
2o	17.0	13.6	16.1	13.4	14.3	13.0

dependent effect on β (-2ω; ω, ω) are stronger than those of β (-ω; ω, 0) for studied complexes. In addition, the order of β_{SHG} and β_{EOPE} values are identical to that the static β_{tot} values: **1c** > **2c** > **1o** > **2o**. The SHG closed/open β_{ratio} are 14.6 and 8.4, whereas the ratios for EOPE are 6.6 and 4.4 within studied complexes. It is obvious that the dynamic ratios are larger than their static counterparts, the trends remain unaltered. Peculiarly, the β (-2ω; ω, ω) values for the complexes **1c** and **2c** at 1340 nm drastically rises up to 568.5×10^{-30} and 144.3×10^{-30} esu, about~ 3.9 times and ~3 times larger than those of corresponding static β_{tot} values. That is attributed to a resonant effect due to the absorption around the second harmonics at 670 nm. It indicates that the second harmonic wavelength should far enough from the absorption bands to avert the overestimation of the β_{tot} values because of resonance effects.

4. Conclusions

In this paper, the first hyperpolarizabilities of a series of mono- and bimetallic Pt(II) DTE-containing complexes were comparatively studied to rationalize the structure-property relationship. Correlating calculations show the introduction of quinolone into the ligand can substantially raise the spatial charge separation, thus improving the second-order NLO responses. On the contrary, Pt(II) complexes containing perfluorocyclopentene ring decrease second-order NLO responses. This series of bimetallic Pt(II) model complexes can be altered by various ligands to control their NLO behaviors. Moreover, the TD-B3LYP calculations present the mixed MLCT/ILCT/LL'CT transitions within the monometal Pt(II) complexes result in the larger first hyperpolarizabilities values than that bimetallic Pt(II) complexes. More interestingly, we give a number of comments on the switching properties of studied complexes. The photoresponse DTE unit is nearly the coplanar structure in closed-ring complexes along with a better π-conjugation, which means a remarkable enhancement of NLO response. The largest β_{tot} contrast (~5.4 times) is found in monometal Pt(II) complexes. The observation is attributed to smaller BLA values and narrowed the energy gap between HOMO and LUMO. We hope this work could be conducive to the perspective for further theoretical and experimental research on rational design for organometallic DTE-based NLO materials.

Acknowledgements

The authors sincerely acknowledge the financial support from “12th Five-Year” Science and Technology Research Project of the Education Department of Jilin Province ([2016] 494).

Appendix A. Supplementary data

Supplementary data related to this article can be found at https://doi.org/10.1016/j.jorganchem.2019.03.009.

References

[1] B.J. Coe, J.A. Harris, L.A. Jones, B.S. Brunschwig, K. Song, K. Clays, J. Garín, J. Orduna, S.J. Coles, M.B. Hursthouse, J. Am. Chem. Soc. 127 (2005) 4845–4859.
[2] G.D. Batema, C.A. van Walree, G.P.M. van Klink, C. de Mello Donegá, A. Meijerink, J. Perez-Moreno, K. Clays, G. van Koten, J. Organomet. Chem. 867 (2018) 246–252.
[3] W.Y. Wang, N.N. Ma, S.L. Sun, Y.Q. Qiu, Phys. Chem. Chem. Phys. 16 (2014) 4900–4910.
[4] M. Shimada, Y. Yamanoi, T. Matsushita, T. Kondo, E. Nishibori, A. Hatakeyama, K. Sugimoto, H. Nishihara, J. Am. Chem. Soc. 137 (2015) 1024–1027.
[5] Y. Shi, L. Xiao, D. Wu, F. Li, D. Li, J. Zhang, S. Li, H. Zhou, J. Wu, Y. Tian, J. Organomet. Chem. 817 (2016) 36–42.
[6] H.Q. Wu, R.L. Zhong, S.L. Sun, H.L. Xu, Z.M. Su, J. Phys. Chem. C 118 (2014) 6952–6958.
[7] M.L.H. Green, S.R. Marder, M.E. Thompson, J.A. Bandy, D. Bloor, P.V. Kolinsky, R.J. Jones, Nature 330 (1987) 360.
[8] H.Y. Wang, L.X. Jing, H.Q. Wang, J.T. Ye, Y.Q. Qiu, J. Organomet. Chem. 869 (2018) 18–25.
[9] C. Dragonetti, A. Colombo, D. Marinotto, S. Righetto, D. Roberto, A. Valore, M. Escadeillas, V. Guerchais, H. Le Bozec, A. Boucekkine, C. Latouche, J. Organomet. Chem. 751 (2014) 568–572.
[10] H.Q. Wang, L. Wang, J.T. Ye, H.M. Xie, Y.Q. Qiu, J. Phys. Chem. C 121 (2017) 28462–28474.
[11] K.A. Green, M.P. Cifuentes, M. Samoc, M.G. Humphrey, Coord. Chem. Rev. 255 (2011) 2530–2541.
[12] G. Grelaud, M.P. Cifuentes, F. Paul, M.G. Humphrey, J. Organomet. Chem. 751 (2014) 181–200.
[13] S. Ishihara, J.P. Hill, A. Shundo, G.J. Richards, J. Labuta, K. Ohkubo, S. Fukuzumi, A. Sato, M.R.J. Elsegood, S.J. Teat, K. Ariga, J. Am. Chem. Soc. 133 (2011) 16119–16126.
[14] B.J. Coe, S. Houbrechts, I. Asselberghs, A. Persoons, Angew. Chem. Int. Ed. 38 (1999) 366–369.
[15] N.N. Ma, S.L. Sun, C.G. Liu, X.X. Sun, Y.Q. Qiu, J. Phys. Chem. A 115 (2011) 13564–13572.
[16] K. Szaciłowski, Chem. Rev. 108 (2008) 3481–3548.
[17] J.E. Green, J. Wook Choi, A. Boukai, Y. Bunimovich, E. Johnston-Halperin, E. Delonno, Y. Luo, B.A. Sheriff, K. Xu, Y. Shik Shin, H.-R. Tseng, J.F. Stoddart, J.R. Heath, Nature 445 (2007) 414.
[18] L. Ordronneau, V. Aubert, V. Guerchais, A. Boucekkine, H. Le Bozec, A. Singh, I. Ledoux, D. Jacquemin, Chem. Eur J. 19 (2013) 5845–5849.
[19] C.E. Powell, M.P. Cifuentes, J.P. Morrall, R. Stranger, M.G. Humphrey, M. Samoc, B. Luther-Davies, G.A. Heath, J. Am. Chem. Soc. 125 (2003) 602–610.
[20] K. Green, N. Gauthier, H. Sahnoune, G. Argouarch, L. Toupet, K. Costuas, A. Bondon, B. Fabre, J.-F. Halet, F. Paul, Organometallics 32 (2013) 4366–4381.
[21] Q.H. Li, K.C. Wu, R.J. Sa, Y.Q. Wei, J. Cluster. Sci. 22 (2011) 365–380.
[22] I. Asselberghs, K. Clays, A. Persoons, A.M. McDonagh, M.D. Ward, J.A. McCleverty, Chem. Phys. Lett. 368 (2003) 408–411.
[23] J. Lin, R.J. Sa, M.X. Zhang, K.C. Wu, J. Phys. Chem. A 119 (2015) 8174–8181.
[24] P.J. Mendes, T.J.L. Silva, M.H. Garcia, J.P.P. Ramalho, A.J.P. Carvalho, J. Chem. Inf. Model. 52 (2012) 1970–1983.
[25] J.P. Malval, I. Gosse, J.P. Morand, R. Lapouyade, J. Am. Chem. Soc. 124 (2002) 904–905.
[26] T.Y. Ma, N.N. Ma, L.K. Yan, T. Zhang, Z.M. Su, J. Phys. Chem. A 117 (2013) 10783–10789.
[27] L.S. Zhang, H.F. Li, Q.Y. Liu, M. Ye, L.Y. Zheng, X.L. Fan, W.Z. Liang, J. Organomet. Chem. 846 (2017) 230–235.
[28] M. Irie, T. Fukaminato, K. Matsuda, S. Kobatake, Chem. Rev. 114 (2014) 12174–12277.
[29] H. Tian, S.J. Yang, Chem. Soc. Rev. 33 (2004) 85–97.
[30] H.L. Wong, N. Zhu, V.W.W. Yam, J. Organomet. Chem. 751 (2014) 430–437.
[31] V. Aubert, V. Guerchais, E. Ishow, K. Hoang-Thi, I. Ledoux, K. Nakatani, H. Le Bozec, Angew. Chem. Int. Ed. 47 (2008) 577–580.
[32] H. Ordronneau, V. Aubert, R. Métivier, E. Ishow, J. Boixel, K. Nakatani, F. Ibersiene, D. Hammoutène, A. Boucekkine, H. Le Bozec, V. Guerchais, Phys. Chem. Chem. Phys. 14 (2012) 2599–2605.
[33] H. Nitadori, L. Ordronneau, J. Boixel, D. Jacquemin, A. Boucekkine, A. Singh, M. Akita, I. Ledoux, V. Guerchais, H. Le Bozec, Chem. Commun. 48 (2012) 10395–10397.
[34] M. Irie, T. Fukaminato, K. Matsuda, S. Kobatake, Chem. Rev. 114 (2014) 12174–12277.
[35] V. Aubert, L. Ordronneau, M. Escadeillas, J.A.G. Williams, A. Boucekkine, E. Coulaud, C. Dragonetti, S. Righetto, D. Roberto, R. Ugo, A. Valore, A. Singh, J. Zyss, I. Ledoux-Rak, H. Le Bozec, V. Guerchais, Inorg. Chem. 50 (2011) 5027–5038.
[36] K.A. Green, M.P. Cifuentes, T.C. Corkery, M. Samoc, M.G. Humphrey, Angew. Chem. 121 (2009) 8007–8010.
[37] J.K.W. Lee, C.C. Ko, K.M.C. Wong, N. Zhu, V.W.W. Yam, Organometallics 26 (2007) 12–15.
[38] D. Espa, L. Pilia, L. Marchiò, M.L. Mercuri, A. Serpe, A. Barsella, A. Fort, S.J. Dalgleish, N. Robertson, P. Deplano, Inorg. Chem. 50 (2011) 2058–2060.
[39] J. Boixel, V. Guerchais, H. Le Bozec, D. Jacquemin, A. Amar, A. Boucekkine, A. Colombo, C. Dragonetti, D. Marinotto, D. Roberto, S. Righetto, R. De Angelis,

J. Am. Chem. Soc. 136 (2014) 5367–5375.
[40] J. Boixel, V. Guerchais, H. Le Bozec, A. Chantzis, D. Jacquemin, A. Colombo, C. Dragonetti, D. Marinotto, D. Roberto, Chem. Commun. 51 (2015) 7805–7808.
[41] J. Boixel, Y. Zhu, H. Le Bozec, M.A. Benmensour, A. Boucekkine, K.M.C. Wong, A. Colombo, D. Roberto, V. Guerchais, D. Jacquemin, Chem. Commun. 52 (2016) 9833–9836.
[42] H. Zhao, E. Garoni, T. Roisnel, A. Colombo, C. Dragonetti, D. Marinotto, S. Righetto, D. Roberto, D. Jacquemin, J. Boixel, V. Guerchais, Inorg. Chem. 57 (2018) 7051–7063.
[43] M.Y. Zhang, C.H. Wang, W.Y. Wang, N.N. Ma, S.L. Sun, Y.Q. Qiu, J. Phys. Chem. A 117 (2013) 12497–12510.
[44] A. Presa, G. Vázquez, L.A. Barrios, O. Roubeau, L. Korrodi-Gregório, R. Pérez-Tomás, P. Gamez, Inorg. Chem. 57 (2018) 4009–4022.
[45] M.J. Frisch, G.W. Trucks, H.B. Schlegel, G.E. Scuseria, M.A. Robb, J.R. Cheeseman, G. Scalmani, V. Barone, B. Mennucci, G.A. Petersson, H. Nakatsuji, M. Caricato, X. Li, H.P. Hratchian, A.F. Izmaylov, J. Bloino, G. Zheng, J.L. Sonnenberg, M. Hada, M. Ehara, K. Toyota, R. Fukuda, J. Hasegawa, M. Ishida, T. Nakajima, Y. Honda, O. Kitao, H. Nakai, T. Vreven, J.A. Montgomery Jr., J.E. Peralta, F. Ogliaro, M. Bearpark, J.J. Heyd, E. Brothers, K.N. Kudin, V.N. Staroverov, T. Keith, R. Kobayashi, J. Normand, K. Raghavachari, A. Rendell, J.C. Burant, S.S. Iyengar, J. Tomasi, M. Cossi, N. Rega, J.M. Millam, M. Klene, J.E. Knox, J.B. Cross, V. Bakken, C. Adamo, J. Jaramillo, R. Gomperts, R.E. Stratmann, O. Yazyev, A.J. Austin, R. Cammi, C. Pomelli, J.W. Ochterski, R.L. Martin, K. Morokuma, V.G. Zakrzewski, G.A. Voth, P. Salvador, J.J. Dannenberg, S. Dapprich, A.D. Daniels, O. Farkas, J.B. Foresman, J.V. Ortiz, J. Cioslowski, D.J. Fox, Gaussian 09, Revision D. 01, Gaussian, Inc., Wallingford CT, 2013.
[46] D. Herebian, K.E. Wieghardt, F. Neese, J. Am. Chem. Soc. 125 (2003) 10997–11005.
[47] W.Y. Wang, L. Wang, N.N. Ma, C.L. Zhu, Y.Q. Qiu, Dalton Trans. 44 (2015) 10078–10088.
[48] C. Adamo, V. Barone, J. Chem. Phys. 110 (1999) 6158–6170.
[49] M. Ernzerhof, G.E. Scuseria, J. Chem. Phys. 110 (1999) 5029–5036.
[50] D. Jacquemin, E.A. Perpète, M. Medved, G. Scalmani, M.J. Frisch, R. Kobayashi, C. Adamo, J. Chem. Phys. 126 (2007), 191108.
[51] T. Yanai, D.P. Tew, N.C. Handy, Chem. Phys. Lett. 393 (2004) 51–57.
[52] J.D. Chai, M. Head-Gordon, Phys. Chem. Chem. Phys. 10 (2008) 6615–6620.
[53] Y. Zhao, D.G. Truhlar, Acc. Chem. Res. 41 (2008) 157–167.
[54] E.G. Hohenstein, S.T. Chill, C.D. Sherrill, J. Chem. Theory Comput. 4 (2008) 1996–2000.
[55] G. Pescitelli, N. Sreerama, P. Salvadori, K. Nakanishi, N. Berova, R.W. Woody, J. Am. Chem. Soc. 130 (2008) 6170–6181.
[56] A. Vlček, S. Záliš, J. Phys. Chem. A 109 (2005) 2991–2992.
[57] M. van Faassen, K. Burke, Phys. Chem. Chem. Phys. 11 (2009) 4437–4450.
[58] R.E. Stratmann, G.E. Scuseria, M.J. Frisch, J. Chem. Phys. 109 (1998) 8218–8224.
[59] J.T. Ye, L. Wang, H.Q. Wang, X.M. Pan, H.M. Xie, Y.Q. Qiu, Theor. Chem. Acc. 137 (2018) 22.